Chemical Engineering Journal 160 (2010) 882–890

Contents lists available at ScienceDirect

Chemical Engineering Journal

journal homepage: www.elsevier.com/locate/cej

Quantitative criteria to define flow patterns in micro-capillaries

Anne-Laure Dessimoz, Pauline Raspail, Charline Berguerand, Lioubov Kiwi-Minsker*

Ecole Polytechnique Fédérale de Lausanne, GGRC, ISIC-SB, Station 6, CH-1015 Lausanne, Switzerland

ARTICLE INFO

Article history:
Received 15 July 2009
Received in revised form 4 November 2009
Accepted 6 January 2010

Keywords:
Microstructure
Multiphase flow
Hydrodynamics
Flow pattern
Dimensionless number
Intensification

ABSTRACT

Hydrodynamics of gas–liquid systems has been studied by high-speed camera. The flow patterns of CO_2/water-based fluids were investigated in three glass microreactors having different geometries. Four main regimes were observed: bubbly, slug, slug–annular and annular flow. The forces being responsible for the pattern formation were quantified using dimensionless numbers: Bond (Bo), Reynolds (Re), Weber (We) and Capillary (Ca) numbers. The study showed that the interfacial tension and the gas inertia are the main forces that drive the interface.

A dimensionless map based on the ratio between the Reynolds and the Capillary numbers of the liquid phase as a function of the Reynolds number of the gas phase was built up for horizontal single channel without heat transfer to rationalise the experimentally observed flow patterns and literature data. Quantitative criteria to predict the slug and the annular flow domain independently on the inlet geometries, reactor material, its cross-section shape and liquid phase properties have been suggested. The criteria can be applied for capillaries with hydraulic diameter from 200 μm up to 3 mm and is an important predictive tool for the rational design of micro-reactors for gas–liquid reactions.

1. Introduction

Miniaturisation of chemical reactors brings several benefits like an effective use of raw materials and energy, higher productivity and inherent safety [1]. Manufacture of chemicals often involves gas–liquid reactions which have been recently tested in microstructured reactors (MSR) [2,3]. However, it is not possible actually to design and control chemical micro-devices for multiphase reactions without a clear knowledge of the flow patterns. The hydrodynamics have a direct influence on the mass and heat transfer characteristics in the MSR.

Gas–liquid hydrodynamics in microchannels is different from the one reported for macro-systems. The complex interaction between gravity, interfacial, viscous and inertial forces is responsible for a variety of flow patterns with regular interfaces [4]. In the case of gas–liquid flow, bubbly, slug (also called plug-flow, Taylor-flow, segmented flow), churn, slug–annular and annular flow can be observed [5]. The main problem for controlling flow pattern is due to its dependence on many experimental parameters like linear velocity, ratio of phases, fluid properties, channel geometry, microreactor material and roughness, pressure and temperature. Indeed, all these parameters influence the relative importance of the different forces. The contribution of the forces can be quantified with dimensionless numbers like Bond, Reynolds, Weber and Capillary numbers. These numbers help to rationalise the experimental results, to develop predictive tools and to understand the flow behaviour [4,6].

Although a lot of results have been reported on gas–liquid flow regimes in horizontal microchannels [7–11], mostly the data were obtained for air–water systems in circular channels and therefore correspond only to a restricted domain [4]. Moreover, no universal flow pattern map exists to correlate the experimentally observed hydrodynamics. Based on the concept that there is a similarity between two-phase flow in microchannels and in large channels at microgravity, Akbar et al. [12] proposed a Weber number-based flow regime map for near circular channel and air–water like fluid pairs. This map predicts well flow transition in channel around 1 mm, but does not work for channels <200 μm [13,14]. Waelchli and von Rohr [15] developed flow pattern maps based on a dimensional analysis for rectangular cross-section microchannels with hydraulic diameter about 200 μm. The map fits well the observed flow patterns but cannot be used to predict the hydrodynamics in circular channel with similar dimension [13]. Hassan et al. [16] proposed universal flow regime map based on superficial velocities for horizontal channels. However, due to the use of velocities as coordinates, the effect of channel diameter and fluid properties is not taken into account. Therefore, experimental studies of flow patterns for different fluids and various microchannel geometries are still needed in order to understand the flow behaviour on the micro-scale and to develop predictive tools.

In the present study, the hydrodynamics of gas–liquid flow was studied for three capillary geometries and various fluid properties.

* Corresponding author. Tel.: +41 21 693 31 82; fax: +41 21 693 60 91.
E-mail address: lioubov.kiwi-minsker@epfl.ch (L. Kiwi-Minsker).

1385-8947/$ – see front matter © 2010 Elsevier B.V. All rights reserved.
doi:10.1016/j.cej.2010.01.011

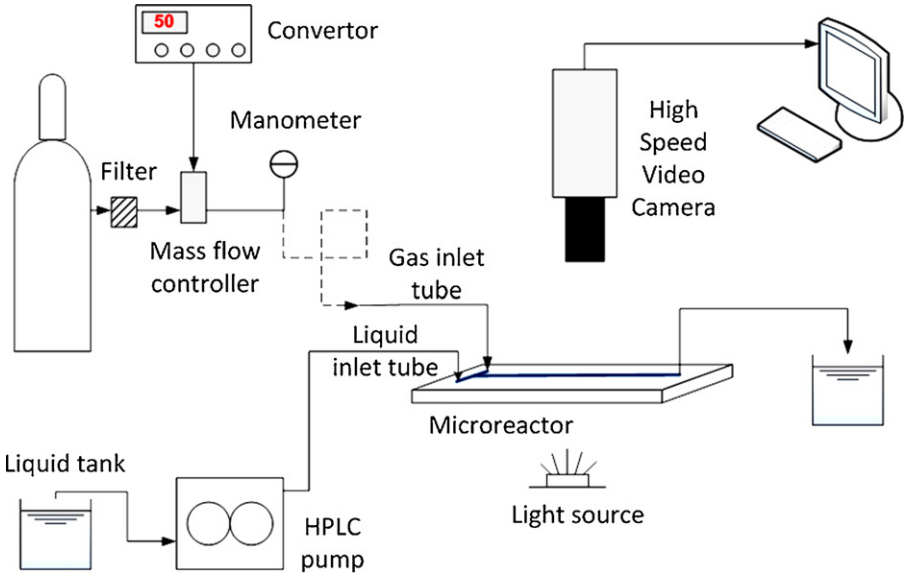

Fig. 1. Scheme of the experimental set-up.

A universal dimensionless map is suggested to predict slug and annular flow regimes in horizontal single channels without heat transfer.

2. Materials and methods

The flow behaviour of CO_2/deionised water system in glass microreactors was investigated with a high-speed camera. The experimental set-up is represented in Fig. 1. Pure CO_2 was convoyed from a gas tank with different mass flow controllers (Bronkhorst High-Tech) to the microreactor. The flow rate was varied between 0.5 and 300 ml/min. At the outlet of the mass flow controller, the pressure was measured by a manometer. For the experiments at low gas velocities, long tubes with small inner diameters (ID 0.2 mm) were added in the gas line to stabilise the flow rate. The liquid phase was supplied by an HPLC pump (model 510 Waters) to the microreactor. The high-speed camera (Videal AG., Olympus BH-2) was used to follow the gas–liquid flow patterns under the experimental conditions. The flow patterns were recorded when the observed flow was stable, which took several minutes. The images were then transferred to a personal computer (Motion Pro Studio® software). All flow patterns reported herein where taken at 3.5 cm distance from the inlet junction over a length of 1.5 cm and the experiments were conducted under ambient conditions (T = 22 °C, P = 1 bar).

2.1. Effect of capillary geometry

The effect of the microreactor geometry on flow patterns was investigated by carrying out experiments in three different glass capillaries (Fig. 2):

(A) T-shaped with square cross-section, hydraulic diameter of 400 μm, length of 56 mm manufactured by the company *Mikroglas*® and named as MKG_Square;
(B) T-shaped with trapezoidal cross-section, hydraulic diameter of 400 μm, length of 237.2 mm, produced by the company *Little Things Factory*® and named as LTF_Trapezoidal;
(C) Y-shaped chicane mixer with circular cross-section, diameter of 1 mm, length of about 250 mm, made by *Little Things Factory*® and named as LTF_Chicane (see Fig. 2 for detailed parameters).

2.2. Effect of liquid phase properties

The influence of liquid physical properties on flow patterns was investigated by adding ethylene glycol, acetone or glycerol to water. The main characteristics of the compounds used during the study are listed in Table 1.

3. Results and discussion

The flow patterns were determined by visual observation of the two-phase flow with a high-speed camera. The images were analyzed and classified in accordance with the flow patterns defined by Triplett et al. [5]. Mostly, four main regimes were observed: bubbly, slug, slug–annular and annular flows. An example for the CO_2/water system is given in Fig. 3.

The bubbly flow, observed at relatively high liquid and medium gas velocities, corresponds to gas bubbles smaller than the channel diameter flowing through the capillary. This flow pattern is rather difficult to stabilise due to gas bubbles coalescence.

The slug flow also called plug-flow, Taylor-flow, bubble train flow or segmented flow occurs for low gas velocity and consists of a succession of bubbles and slugs with diameters equal to the channel. To increase the accuracy of the study, three sub-categories in the slug flow regime were distinguished:

- the stable slug flow which consists of a stable train of bubbles and liquid slugs;
- the irregular slug flow characterised by some variations in bubble and slug length;
- the unstable slug flow, also observed by Yue et al. [14], which corresponds to irregular and coalescing bubbles.

With an increase of the gas velocity, the slugs merge and a new flow pattern is created, known as slug–annular flow. Finally, at very high gas velocity, the annular flow appears. It corresponds to a flowing gas core and a wetting phase confined to the wall. The churn flow as described by Triplett et al. [5] was never observed in the present study.

The most common flow regimes are the slug and annular flow being important due to a constant and uniform interfacial area. Unstable slug flow appears as a mix between slug flow and slug–annular flow. Slug–annular regime can be defined as an annular flow which is no more stable.

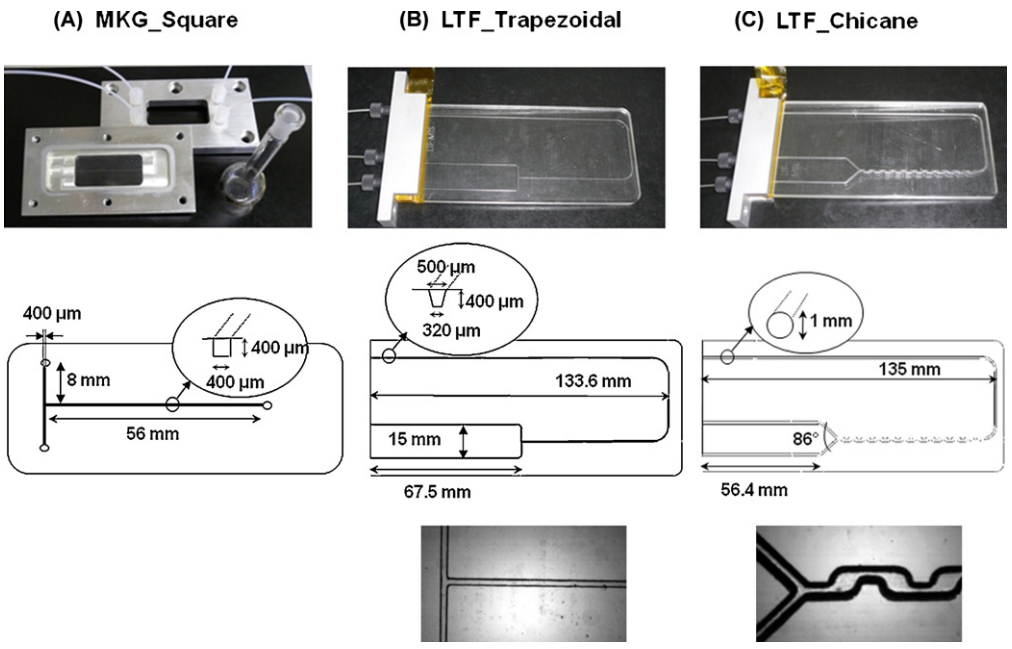

Fig. 2. Glass microreactors used during the present study. (A) MKG_Square. (B) LTF_Trapezoidal. (C) LTF_Chicane.

Table 1
Purity and physical properties of the compounds used [20].

Substances		Conc.	Density ρ at 20 °C [kg/m^3]	Viscosity μ at 20 °C [Pa s]	Interfacial tension fluid/air (T °C) [N/m]	Interfacial tension fluid/CO_2 (T °C) [N/m] [21]
CO_2	Carbagas	99.5%	1.799	1.50×10^{-5}		
Water	Deionised	–	998.2	1.002×10^{-3}	7.28×10^{-2} (20)	7.2×10^{-2} (20)
Acetone	Technical quality	3 wt%	994.0	1.072×10^{-3}	6.39×10^{-2} (25)	
Ethylene glycol	>99.5% standard, Fluka®	10 wt%	1010.8	1.277×10^{-3}	6.85×10^{-2} (20)	
Ethylene glycol		16 wt%	1018.8	1.5×10^{-3}	6.62×10^{-2} (20)	
Glycerol	100% standard for analysis, Acros Organics®	20 wt%	1045.9	1.737×10^{-3}	6.95×10^{-2} (25)	

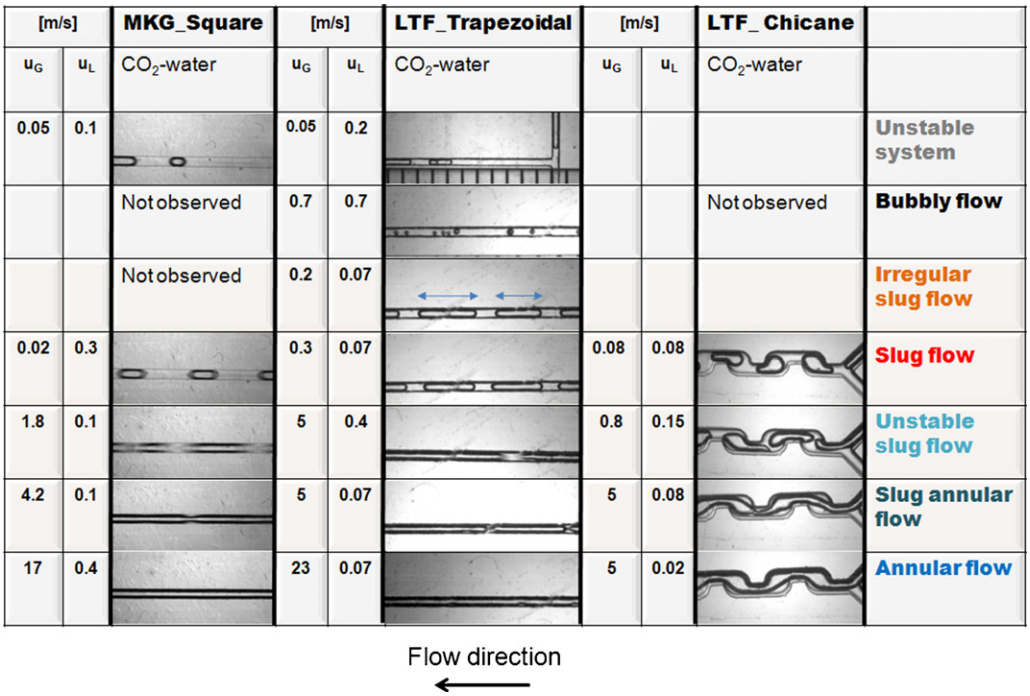

Fig. 3. Flow patterns observed in the three glass microreactors as a function of the gas and liquid linear velocities.

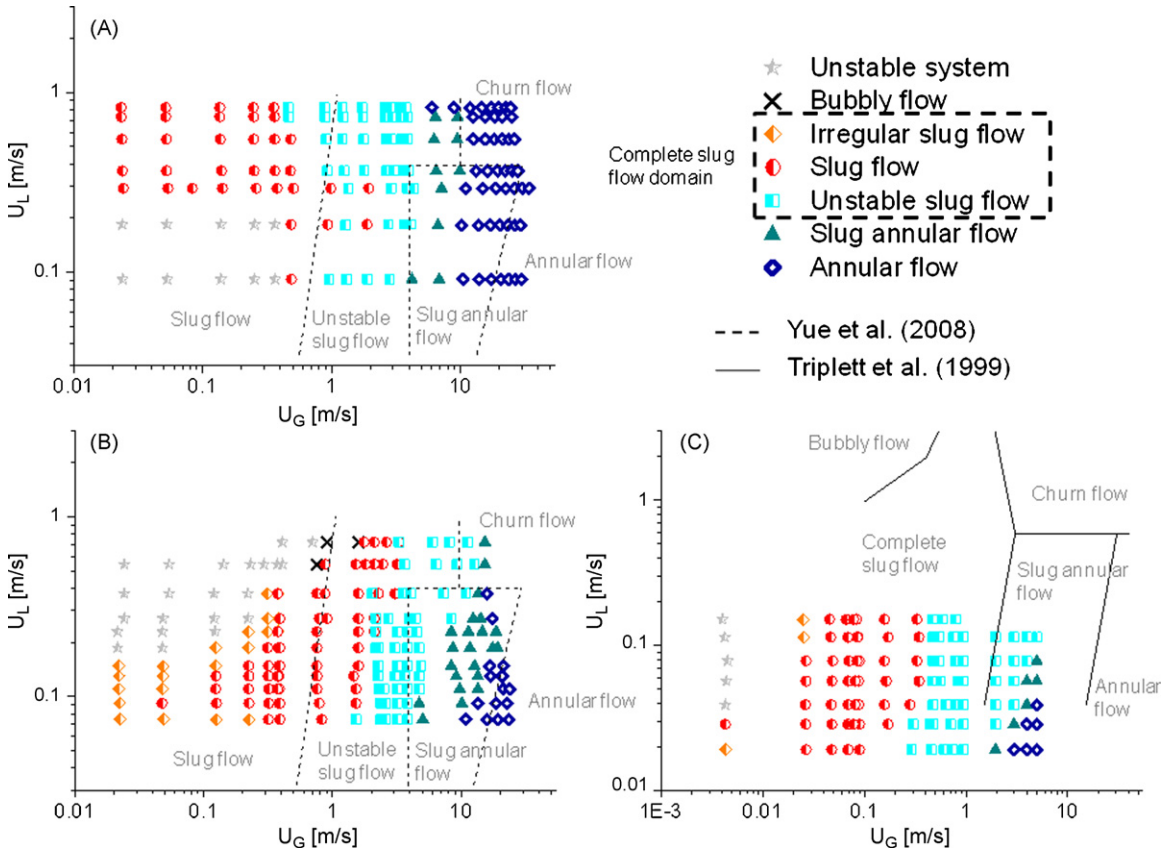

Fig. 4. Effect of reactor geometry on flow patterns transitions for the CO_2–water fluid system. (A) MKG_Square. (B) LTF_Trapezoidal. (C) LTF_Chicane.

The different flow regimes were presented as flow pattern maps with the gas and liquid superficial velocities as coordinates.

$$u_i = \frac{Q_i}{A}, \qquad i = G, L \tag{1}$$

where u [m/s] is the superficial velocity, Q [m^3/s] the volumetric flow rate and A [m^2] the channel cross-section. The subscripts correspond to the gas and liquid phases, respectively.

All gas superficial velocities reported herein correspond to the local values in the observation window (3.5 cm distance from the inlet junction). The pressure drop was measured and the pressure at the inlet of the microreactor was determined. The pressure at the position where the images were recorded was calculated based on a linear distribution of the pressure drop as a function of the length and was used to derive the local superficial velocity.

In the maps (see Fig. 4), experimentally determined flow patterns are marked differently and the transitions boundaries of one flow pattern to the other are indicated by lines. The stars represent the unstable domain.

3.1. Effect of reactor geometry

Based on comparisons with literature data, Waelchli and von Rohr [15] suggested that the impact of cross-sectional channel shape is more important than the hydraulic diameter for the formation of the flow patterns. Indeed, the flow in circular and non-circular channels may be very different due to the presence of sharp corners [17]. At contrast, Triplett et al. [5] demonstrated that the flow pattern transition lines are very similar in circular and semi-triangular channels. Therefore, to solve this discrepancy, the effect of the cross-section shape on flow patterns was investigated in details.

The flow pattern maps experimentally obtained for the MKG_Square and LTF_Trapezoidal microreactors with the same hydraulic diameter but different cross-section shapes are shown in Fig. 4A and B, respectively. The indicated transition lines correspond to those reported by Yue et al. [14] and are used as a reference in the present study because the authors tested the same fluid system (CO_2/water) in a similar microchannel as the MKG_Square. Their microreactor is a Y-junction PMMA capillary, with a hydraulic diameter of 400 μm and a square cross-section. Therefore, the main differences between MKG_Square and the reactor used by Yue et al. [14] are the inlet geometry and microchannel material. The inlet geometry was recognised to have a major impact on the transition from slug to bubbly flow but not on other patterns [13]. Therefore, this transition between bubbly and slug flow was not considered when comparing with our experimental results.

The flow patterns obtained with the MKG_Square fit quite well with the transition lines of Yue et al. [14], especially for the transitions from slug to unstable slug flow and from unstable slug flow to slug-annular flow. However, in the case of the trapezoidal cross-section (LTF_Trapezoidal) the transition between stable and unstable slug flow cannot be predicted anymore by the transition lines of Yue et al. [14]. In conclusion, the cross-section shape influences mainly the stable slug flow domain and has little impact on the transition to slug–annular flow. This particular fact was not recognized by Triplett et al. [5] as no distinction was done between the stable and unstable slug flow regimes.

At contrast, the annular flow domain obtained in the MKG_Square is different from the ones observed in the LTF_Trapezoidal and by Yue et al. [14]. A possible explanation could be the combined effect of the microchannel material and cross-section shape on annular flow regime stabilisation. The PMMA is hydrophobic, whereas the untreated glass is hydrophilic. Therefore,

we suppose that the glass material helps to stabilise the annular flow in the MKG_Square compared to PMMA [14]. Moreover, the trapezoidal cross-section (LTF_Trapezoidal) is certainly less suitable than the square one to stabilise the annular flow regime due to decrease of the symmetry of the film. However, the experimental error in the determination of this flow pattern cannot be excluded since it is sometimes difficult to distinguish slug–annular and annular flow.

Apart from the diameter and channel cross-section, the influence of non-straight channels on the flow patterns is important [6], but only few data are reported. The flow pattern map for the LTF_Chicane and the transition lines reported by Triplett et al. [5] for a straight microchannel with circular cross-section of 1.1 mm are plotted in Fig. 4C. As can be observed, the transition lines quite accurately determine the complete slug flow domain. The results suggest that the meander does not affect greatly the two-phase flow behaviour.

3.2. Effect of liquid phase properties on flow patterns

To change the liquid phase properties 3 wt% of acetone and 16 wt% of ethylene glycol were added to water. In Fig. 5A and B, the flow pattern maps are shown for the LTF_Trapezoidal and MKG_Square microreactor, respectively. The transition lines correspond to the CO_2–water system (reference fluid system). As indicated in Table 1, the addition of acetone in water decreases the interfacial tension and the addition of ethylene glycol increases the viscosity as compared to the reference system. Based on these experimental results, general trends about the effect of liquid phase properties on flow patterns in microchannels can be highlighted.

The decrease of interfacial tension extends the bubbly flow domain to lower gas velocities (Fig. 5A) and stabilise of the slug annular flow at high liquid flow rates. The increase of liquid viscosity (Fig. 5B) helps to obtain slug–annular flow and annular flow at lower gas velocity. No effect of the liquid phase properties on the transition between slug and unstable slug flow has been observed. An increase of the liquid viscous forces helps to destabilise the shape of the bubbles and to obtain the gas core with the liquid at the wall (annular flow).

3.3. Dimensionless analysis

In the case of two-phase flows in microreactors the interfacial tension, the inertia and the viscosity are the most important forces controlling the interface. The relative importance of these three forces can be characterised by the Reynolds, Weber and Capillary dimensionless numbers [4].

The Reynolds number defines the ratio between inertial and viscous forces:

$$\mathrm{Re} = \frac{\rho \cdot u \cdot d_H}{\mu} \tag{2}$$

where d_H [m] is the hydraulic diameter of the channel, ρ [kg/m^3] is the fluid density and μ [Pa s] the dynamic fluid viscosity.

The Weber number represents the ratio between inertial and interfacial forces:

$$\mathrm{We} = \frac{u^2 \cdot d_H \cdot \rho}{\sigma} \tag{3}$$

where σ [kg/s^2] is the interfacial tension between gas and liquid.

The Capillary number defines the ratio between viscous and interfacial forces:

$$\mathrm{Ca} = \frac{\mu \cdot u}{\sigma} \tag{4}$$

The Capillary number can also be determined by dividing the Weber number by the Reynolds number. Moreover, the importance of gravity with respect to interfacial forces is described by the Bond number [4]:

$$\mathrm{Bo} = \frac{(\Delta\rho) \cdot g \cdot d_H^2}{\sigma} \tag{5}$$

where $\Delta\rho$ [kg/m^3] is the density difference between the liquid and the gas, and g [m/s^2] is the gravitational acceleration. When the interfacial forces dominate over gravity, the Bond number is <1.

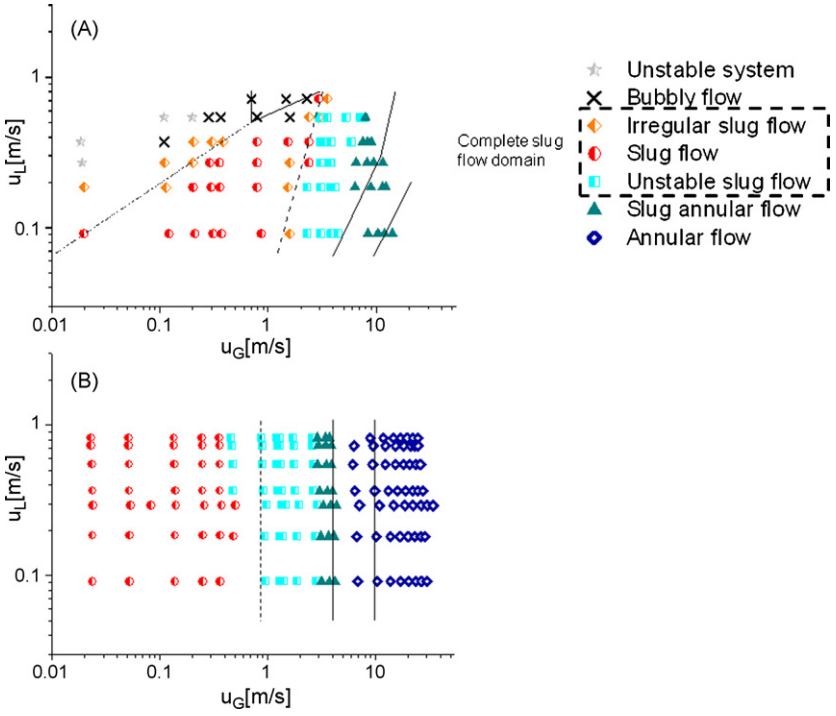

Fig. 5. Effect of liquid phase properties on flow patterns transition. (A) Water + acetone 3 wt%–CO_2 with the transition lines for the CO_2/water system in the LTF_Trapezoidal microreactor. (B) Water + EG 16 wt%–CO_2 with the transition lines for the CO_2/water system in the MKG_Square.

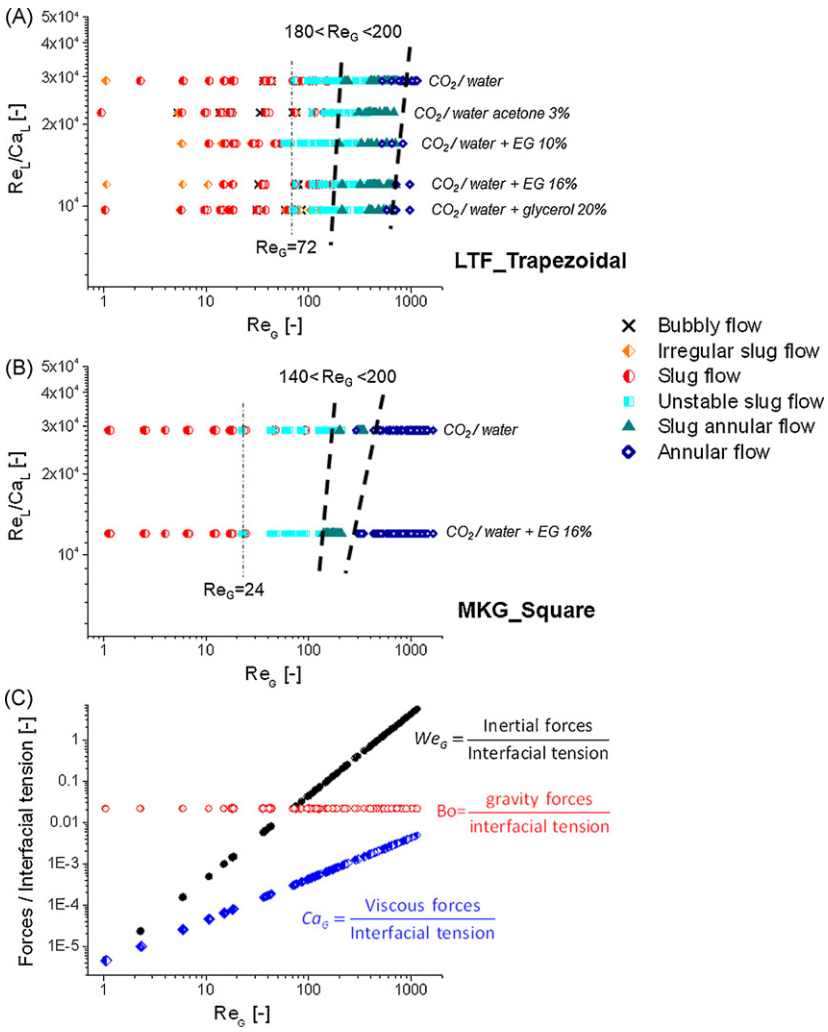

Fig. 6. (A) Dimensionless map for the LTF_Trapezoidal microreactor. (B) Dimensionless map for the MKG_Square microreactor. (C) We_G, Bo and Ca_G as a function of the Re_G.

Moreover, all forces are balanced when We, Ca and Bo are close to 1.

Assuming that the hydrodynamics is mainly governed by interfacial tension, inertia and viscosity, a suitable flow pattern map should be obtained by combining phasic Reynolds and Capillary numbers (or phasic Reynolds and Weber numbers).

Jayawardena et al. [18] made experiments under microgravity and correlated successfully the observed flow patterns using two dimensionless groups. The first group is the ratio of the Reynolds to the Capillary numbers for the liquid phase and represents the product of surface tension and inertia forces to the square of the viscous forces (Eq. (6)).

$$\frac{\mathrm{Re_L}}{\mathrm{Ca_L}} = \frac{\rho_L \cdot d_H \cdot \sigma}{\mu_L^2} \tag{6}$$

The second group is the Reynolds number of the gas phase (Re_G). One advantage of this map is that all liquid physical properties are taken into account by the Re_L/Ca_L ratio. Moreover, the effect of the gas phase is described by Re_G.

In the present study, for the first time a similar analysis was applied to microreactors. In Fig. 6A and B, all flow patterns experimentally observed with the different fluid systems, in the LTF_Trapezoidal and in the MKG_Square, are plotted as a function of two dimensionless groups, Re_L/Ca_L and Re_G. The dimensionless numbers were calculated based on the interfacial tension between the studied liquid and air (Table 1) because the values are similar to CO_2. Two bold dashed lines were drawn to distinguish between the complete slug flow, the intermediate (mainly slug–annular domain) and the annular flow domain. The third thin dashed line determines the stable slug flow domain. These maps allow rationalising the experimental results and can be used to predict the slug and annular flow regimes in the microreactors studied for different fluid properties.

As seen from the figures, the transition line between stable slug flow and unstable slug flow strongly depends on the geometry of the microreactor but is not influenced by liquid phase properties. Therefore, the following criteria can be applied to distinguish the stable slug flow in the two different geometries:

$$\begin{array}{l}\text{STABLE SLUG FLOW}\\ \text{Square cross-section} \Rightarrow \quad \mathrm{Re_G} < 24\\ \text{Trapezoidal cross-section} \Rightarrow \mathrm{Re_G} < 72\end{array} \tag{7}$$

Concerning the transition lines between the complete slug flow domain and the slug annular domain only small effects of liquid phase properties and channel geometry were observed. The transition zone corresponds to $140 < Re_G < 200$ independently of the reactor geometry and liquid phase properties.

For the transition to annular flow, different tendencies were observed between the two microreactors. The determination of quantitative criteria is not straightforward. The experimental results will be compared with the literature in Section 3.4 in order to highlight general tendencies.

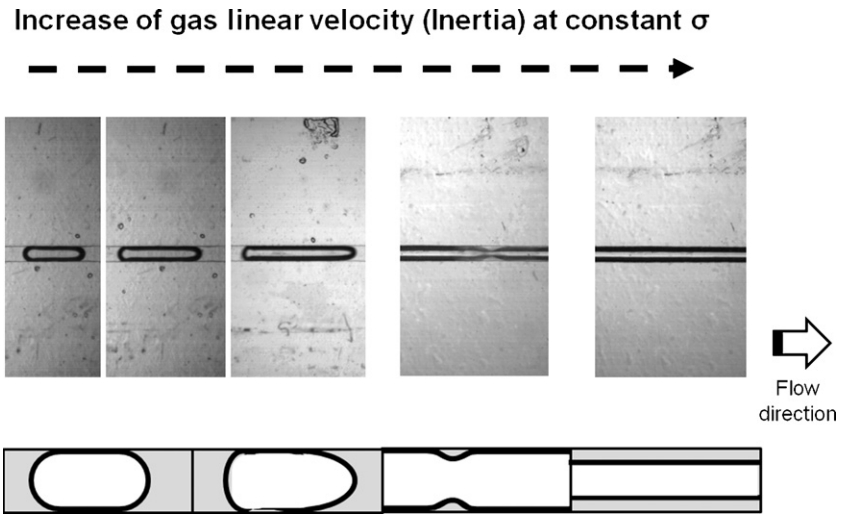

Fig. 7. Effect of inertia on flow patterns at constant interfacial tension.

In Fig. 6C, the different forces related to the interfacial tension (We_G, Bo and Ca_G) are plotted as a function of the Reynolds number of the gas phase (Re_G). The graph corresponds to both geometries as the hydraulic diameter is the same. Moreover, for the calculation of We_G, Bo and Ca_G the CO_2/water system was considered. In this way, the relative importance of the different forces can be analyzed and linked to the observed flow patterns (Fig. 6A and B). As is seen, in microreactors the surface tension dominates over gravity (Bo < 1) and the ratio does not depend on the Reynolds number. Apart from the interfacial tension, the other important force is the inertia. When We_G (ratio of inertia to interfacial forces) is small the slug flow is obtained in both reactor geometries due to the predominance of surface tension. At high liquid velocity, some bubbly flow can also be observed. On the opposite, when the We_G is large, the inertia exceeds the interfacial tension and the annular flow is observed, independently on the reactor geometry or liquid phase properties.

The major influence of inertia on flow patterns can be relatively simply explained (Fig. 7). The bubbly and slug flow can be observed when the interfacial tension dominates over inertia. In this case, the interfacial forces maintain the hemispherical shape of the bubble. With the increase of the gas linear velocity (increase of the relative influence of inertia), the nose of the bubble is elongated and the rear flattened [19], which leads to the transition to slug–annular flow. When the inertia starts to dominate, the annular flow is formed. Therefore, the main parameter which governs the transition between slug flow and annular flow is the gas linear velocity and this justifies the use of a flow pattern map based on Re_G.

3.4. Validation of the criteria based on literature data

The experimental results for the three different geometries and various liquid properties were compared with the literature data. The flow pattern maps of Yue et al. [14] for Y-junction PMMA microchannels having hydraulic diameters of 667, 400 and 200 μm, the maps of Triplett et al. [5] for circular and semi-triangular cross-section microchannels with 1.1 mm inner diameters, the maps of Yang and Shieh [11] for air–water flow in horizontal circular tubes with inside diameter of 1–3 mm and the map of Chung and Kawaji [7] for nitrogen gas and water in circular channel of 0.53 mm diameter were considered. Table 2 summarises the different studies and experimental conditions. Our attempts to find a quantitative criteria using the universal maps of Akbar et al. [12] and Hassan et al. [16] based on superficial velocities failed specially for the channels with small diameters and trapezoidal cross-sections.

Table 2
Literature data for adiabatic gas–liquid flow in horizontal micro/mini channels under ambient conditions.

	No.	Fluid system	Inlet	Material	d_H [mm]	Cross-section
Triplett et al. [5]	1 2	Air/water	Cross-component mixer	Pyrex Acrylic (PMMA)	1.1 1.09	Circular Semi-triangular
Yang and Shieh [11]	1 2 3	Air/water	Mixer with mesh filter	Pyrex	1 2 3	Circular
Akbar et al. [12]			Universal map		≤1	Near circular
Chung and Kawaji [7]		N_2/water	Mixer	Silica with coating	0.53	Circular
Hassan et al. [16]			Universal map for horizontal microchannels			
Yue et al. [14]	1 2 3	CO_2/water	Y-junction	PMMA	0.2 0.4 0.667	Square Square Rectangular
Present study—LTF_Trapezoidal	1 2	CO_2/water CO_2/water + glycerol 20%	T-junction	Glass	0.4	Trapezoidal
Present study—MKG_Square	1 2	CO_2/water CO_2/water + EG 16%	T-junction	Glass	0.4	Square
Present study—LTF-Chicane		CO_2/water	Y-junction	Glass	1	Circular

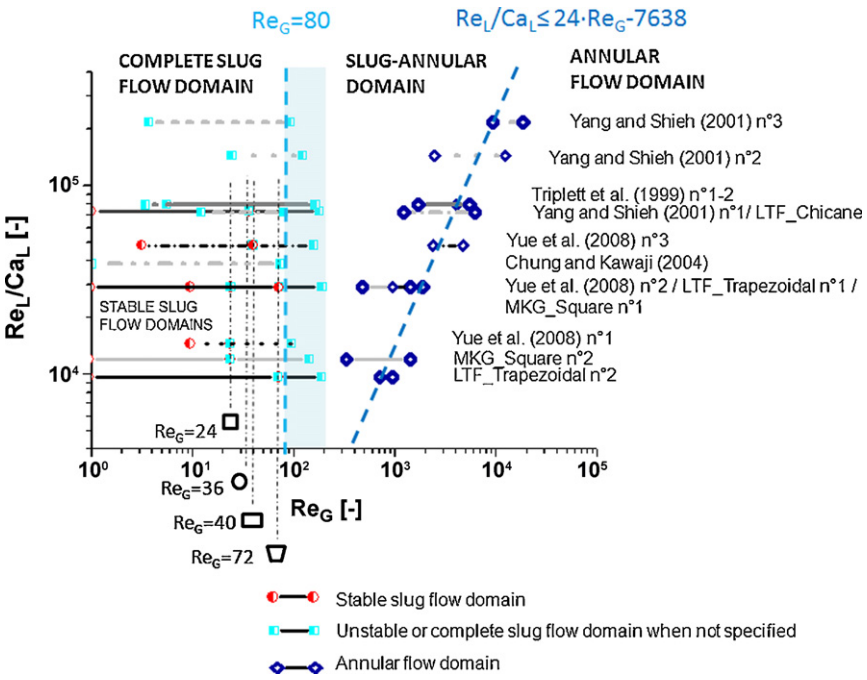

Fig. 8. Universal dimensionless map.

Therefore, we build up a general dimensionless map based on the ratio Re_L/Ca_L as a function of Re_G using all data available (Fig. 8). The flow patterns were considered only for liquid superficial velocities smaller that 0.5 m/s. It means that the unstable bubbly and churn flow were not taken into account. Indeed, operating conditions for gas–liquid reactions are typically at low liquid velocity (u_L < 0.1 m/s) [4]. Therefore, for each study, the domains corresponding to the stable slug flow, the unstable slug flow or complete slug (when no distinctions was done) and annular flow were plotted as a function of the Reynolds number of the gas phase.

As seen from Fig. 8, the stable slug flow domain (represented by the thin dashed lines) depends only on the cross-section geometry of the microchannel. This transition line is independent on the channel diameter, liquid properties, inlet geometries and channel material. For example, the results of Yue et al. [14] for the square capillaries of 0.2 and 0.4 mm are in perfect agreement with our experimental data for the MKG_Square. Based on the data for the circular channel (LTF_Chicane) and for the rectangular microchannel investigated by Yue et al. [14], two other criteria were introduced: for circular channels Re_G < 36 and for rectangular channels Re_G < 40.

As have been seen in Section 3.3, the complete slug flow domain depends slightly on the geometry and liquid phase properties. Based on Fig. 8, a simple criterion can be applied to predict the complete slug flow domain: Re_G < 80. Indeed, the transition zone is always between Re_G 80 and 200 for all data reported. Apart from the effect of the geometry and liquid phase properties, the variation can be attributed to the difficulty of the visual determination of the flow patterns and the absence of a universal classification.

$$\begin{aligned}&\text{STABLE SLUG FLOW DOMAIN}\\&\text{Square cross-section} \Rightarrow \quad Re_G < 24\\&\text{Circular cross-section} \Rightarrow \quad Re_G < 36\\&\text{Rectangular cross-section} \Rightarrow \quad Re_G < 40 \quad (\text{aspect ratio} = 2)\\&\text{Trapezoidal cross-section} \Rightarrow \quad Re_G < 72\end{aligned} \tag{8}$$

$$\text{COMPLETE SLUG FLOW DOMAIN} \Rightarrow Re_G < 80$$

Analysis of the data obtained in this study and reported in the literature shows that a correlation based on Re_L/Ca_L and Re_G (Fig. 8) is also valid to predict the annular flow domain:

$$\text{ANNULAR FLOW DOMAIN} \Rightarrow \frac{Re_L}{Ca_L} \leq 24 \cdot Re_G - 7638 \tag{9}$$

This correlation corresponds to the limit where annular flow can be observed for all reported operating conditions. It reflects the influence of viscosity and channel diameter on the annular flow pattern. Moreover, it predicts the disappearance of the slug–annular domain for the channels with small hydraulic diameters. The variation in the reported results could be attributed to the various geometries, material, liquid properties, diameters and inlet properties. Nevertheless, the experimental error should also play a significant role.

Therefore, it can be concluded that that the criteria (Eqs. (8) and (9)) are suitable to predict the slug and annular flow domain, independently on the inlet geometries, reactor material, cross-section shape and liquid phase properties and can be applied for hydraulic diameter between 200 μm and 3 mm. Moreover, these criteria are also suitable for non-straight geometries (circular LTF_Chicane).

4. Conclusions

- The flow of CO_2/water-based fluids was investigated by a high-speed camera in three glass capillaries having different geometries. Four main regimes were observed: bubbly, slug (including three sub-regimes: irregular slug flow, stable slug flow and unstable slug flow), slug–annular and annular flow.
- Two dimensionless maps were developed for the square and trapezoidal cross-section microreactors, based on the ratio between the Reynolds and the Capillary numbers of the liquid phase as a function of the Reynolds number of the gas phase.
- The relative importance of the different forces (interfacial tension, gravity, inertia, viscosity) was analyzed and linked to the observed flow patterns. Interfacial tension and inertia were recognized as the main forces that determine the flow patterns.

- Quantitative criteria to predict the slug and the annular flow domain independently on the inlet geometries, reactor material, cross-section shape and liquid phase properties were suggested. The criteria can be applied for microchannels with hydraulic diameter from 200 μm up to 3 mm. The results have particular importance for the rational design of microreactors.

Acknowledgements

The authors thank Prof. Albert Renken for fruitful discussions. Financial support by the Swiss National Science Foundation and the Swiss Commission for Technology and Innovation (CTI) is highly appreciated.

References

[1] L. Kiwi-Minsker, A. Renken, Microstructured reactors for catalytic reactions, Catal. Today 110 (2005) 2–14.
[2] V. Hessel, P. Angeli, A. Gavriilidis, H. Lowe, Gas–liquid and gas–liquid–solid microstructured reactors: contacting principles and applications, Ind. Eng. Chem. Res. 44 (2005) 9750–9769.
[3] K. Jahnisch, V. Hessel, H. Lowe, M. Baerns, Chemistry in microstructured reactors, Angew. Chem. Int. Ed. 43 (2004) 406–446.
[4] A. Gunther, K.F. Jensen, Multiphase microfluidics: from flow characteristics to chemical and materials synthesis, Lab Chip 6 (2006) 1487–1503.
[5] K.A. Triplett, S.M. Ghiaasiaan, S.I. Abdel-Khalik, D.L. Sadowski, Gas–liquid two-phase flow in microchannels—Part I: Two-phase flow patterns, Int. J. Multiphase Flow 25 (1999) 377–394.
[6] V. Hessel, A. Renken, J.C. Schouten, J.-I. Yoshida (Eds.), Handbook of Micro Reactors: Chemistry and Engineering, Wiley–VCH, 2009.
[7] P.M.Y. Chung, M. Kawaji, The effect of channel diameter on adiabatic two-phase flow characteristics in microchannels, Int. J. Multiphase Flow 30 (2004) 735–761.
[8] T. Cubaud, C.M. Ho, Transport of bubbles in square microchannels, Phys. Fluids 16 (2004) 4575–4585.
[9] R. Pohorecki, P. Sobieszuk, K. Kula, W. Moniuk, A. Zielinski, P. Cyganski, P. Gawinski, Hydrodynamic regimes of gas–liquid flow in a microreactor channel, Chem. Eng. J. 135 (2008) S185–S190.
[10] S. Saisorn, S. Wongwises, Flow pattern, void fraction and pressure drop of two-phase air–water flow in a horizontal circular micro-channel, Exp. Therm. Fluid Sci. 32 (2008) 748–760.
[11] C.Y. Yang, C.C. Shieh, Flow pattern of air–water and two-phase R-134a in small circular tubes, Int. J. Multiphase Flow 27 (2001) 1163–1177.
[12] M.K. Akbar, D.A. Plummer, S.M. Ghiaasiaan, On gas–liquid two-phase flow regimes in microchannels, Int. J. Multiphase Flow 29 (2003) 855–865.
[13] N. Shao, A. Gavriilidis, P. Angeli, Flow regimes for adiabatic gas–liquid flow in microchannels, Chem. Eng. Sci. 64 (2009) 2749–2761.
[14] J. Yue, L.G. Luo, Y. Gonthier, G.W. Chen, Q. Yuan, An experimental investigation of gas–liquid two-phase flow in single microchannel contactors, Chem. Eng. Sci. 63 (2008) 4189–4202.
[15] S. Waelchli, P.R. von Rohr, Two-phase flow characteristics in gas–liquid microreactors, Int. J. Multiphase Flow 32 (2006) 791–806.
[16] I. Hassan, M. Vaillancourt, K. Pehlivan, Two-phase flow regime transitions in microchannels: a comparative experimental study, Microscale Thermophys. Eng. 9 (2005) 165–182, Cited by [13].
[17] P.M.Y. Chung, M. Kawaji, A. Kawahara, Y. Shibata, Two-phase flow through square and circular microchannels—effects of channel geometry, J. Fluids Eng. Trans. ASME 126 (2004) 546–552.
[18] S.S. Jayawardena, V. Balakotaiah, L.C. Witte, Pattern transition maps for microgravity two-phase flows, AlChE J. 43 (1997) 1637–1640.
[19] M.T. Kreutzer, F. Kapteijn, J.A. Moulijn, C.R. Kleijn, J.J. Heiszwolf, Inertial and interfacial effects on pressure drop of Taylor flow in capillaries, AlChE J. 51 (2005) 2428–2440.
[20] D.R. Lide (Ed.), CRC Handbook of Chemistry and Physics, 89th Edition (Internet Version 2009) CRC Press: Boca Raton, FL, 2008–2009.
[21] A. Hebach, A. Oberhof, N. Dahmen, A. Kogel, H. Ederer, E. Dinjus, Interfacial tension at elevated pressures—measurements and correlations in the water plus carbon dioxide system, J. Chem. Eng. Data 47 (2002) 1540–1546.